Article:
Mahmoud, BH, Mortimer, LF, Fairweather, M et al. (3 more authors) (2020) Multiscale modelling of ceramic nanoparticle interactions and their influence on the thermal conductivity of nanofluids. Journal of Physics D: Applied Physics, 53 (1). 015501. ISSN 0022-3727

https://doi.org/10.1088/1361-6463/ab45ce

Multiscale modelling of ceramic nanoparticle interactions and their influence on the thermal conductivity of nanofluids

Bashar H. Mahmoud [a], Lee F. Mortimer [a], Michael Fairweather [a], Jeffrey Peakall [b], David Harbottle [a], Hugh P. Rice [a]*

[a] School of Chemical and Process Engineering, and [b] School of Earth and Environment, University of Leeds, Leeds LS2 9JT, UK

*bgy9bm@leeds.ac.uk

KEYWORDS: Nanofluids, ceramic nanoparticles, aggregation, thermal conductivity, thermal energy storage

ABSTRACT

There is currently a lack of a reliable theory capable of making accurate predictions of the thermal enhancement in nanofluids (with relatively low solid volume fractions). The work described therefore assesses the thermal conductivity of nanoparticle suspensions in fluids using a Lagrangian particle tracking-based computational modelling technique. A three-dimensional, multiphase fluid-solid model is developed which predicts the motion of suspended nanoparticles. The nanofluid is predicted using an Eulerian-Lagrangian hybrid approach with a constant timestep. This technique takes various multiscale forces into consideration in the calculations, whose characteristic scales are quite different, providing for the first time an analysis of all factors affecting the stability and thermal conductivity of nanofluids. The system considered consists of 71 nm diameter Al_2O_3 ceramic nanoparticles suspended in water, with homogeneous temperature distributions ranging from 25 to 85°C, at various volume fractions between 1 and 5%. The results of the simulations demonstrate the effectiveness of the presented technique, with predictions

elucidating the role of Brownian motion, fluid viscous drag, inter-particle collisions and DLVO attraction and repulsion forces on nanofluid stability. Results indicate that aggregated nanoparticles formed in the suspensions, at various particle concentrations, play an important role in the thermal behaviour of the nanofluids. Predictions are in agreement with theoretical and experimental results obtained in related studies. The thermal characteristics of nanofluids are also considered as a function of temperature, system chemistry and time (measured from an initially homogeneously dispersed state). The proven enhancement in the conductivity of fluids affected by the addition of nanoparticles has great potential to assist the development of commercial nanofluid technology aimed at energy efficient and sustainable processes.

INTRODUCTION

The growing interest in energy efficient and sustainable technologies has created significant demand for novel heat transfer and thermal energy storage materials, such as hybrid nanofluids. The importance of nanoscience cannot be underestimated here, since the motivation for the manipulation, through nanoparticle addition, of the properties of existing thermal fluids (e.g. water, oil, ethylene glycol and molten salt) arises from their poor thermal properties which represents a major limitation to the development of more energy efficient processes. New concepts were suggested by Choi[1] to improve the heat transfer properties of classical conductive fluids through the addition of small concentrations of various sized nanoparticles, between 10 and 100 nm in diameter. Work in this field has since received increased attention, with extensive experimental, theoretical and computational research having been performed[2-5]. Heat transfer characteristics reported in the literature have been obtained using different types of nanoparticles such as metal oxides, non-metallic and carbon nanotubes, with substantially higher values of thermal conductivity, k, observed. The most significant enhancement is for fluids containing ceramic

nanoparticles such as aluminium oxide (Al_2O_3) in water with volume fractions ranging between 1 and 5%, for which increases in k of between 2 and 36% have been obtained[1-4].

For nanofluids, different mechanisms and models have been proposed to explain the dramatic increase in thermal conductivity, especially at low nanoparticle loadings. The methods proposed by various investigators can broadly be divided into two categories: (i) static mechanisms (based on the structure of the stationary dispersion of solid nanoparticles in the liquid medium); and (ii) dynamic mechanisms (which consider the kinetics and random movement and interactions of nanoparticles in the liquid medium). The first category, as described by Wang and Mujumdar[2], explains thermal transport in nanofluids through classical effective medium theories[5-9], the nanoscale layer between the fluid and the nanoparticle interface[10-12], and the aggregation or clustering of nanoparticles[13-15]. Assumptions are made for the transport of heat in each phase based on the diffusion equation, which may only work for low conductivity ratios (~10) between the solid and the fluid[16]. As a result, when mathematical models based on this approach are used to predict nanofluid properties at low volume fractions, they tend to underestimate measured thermal conductivity values[17]. This explains why most static models fail to sufficiently describe the thermal conductivity of nanofluids, if they are used alone.

The second category considers the continuous movement of the nano-sized particles with respect to time, and between the fluid molecules, under certain thermodynamic conditions, including collisions between nanoparticles[10, 18] and their Brownian motion[19]. Enhancements in thermal conductivity are explained using four mechanisms: (i) collision of the base fluid molecules with each other; (ii) thermal diffusion of nanoparticles within the fluid; (iii) collision of nanoparticles with each other; and (iv) Brownian motion-induced nano-convection of particles (as a secondary dynamic mechanism). Further details of each of these mechanisms, and models of them, are given

by Lee and Jang[17]. However, the disparities between experimental conductivity data and model predictions suggests that conventional heat conduction models, developed for multiphase fluids containing larger particles (three to six orders of magnitude in diameter greater than nanoparticles) are inadequate for nanofluids, as detailed by Das et al.[20]. The current lack of a reliable theory capable of making accurate predictions of the thermal enhancement in nanofluids (with relatively low solid volume fractions) is therefore evident, as reported by Wang and Mujumdar[2].

With the aim of overcoming this issue, many researchers have tried to combine the static and dynamic mechanisms of thermal conductivity enhancement in nanofluids. Among the first to undertake such work were Ren et al.[21] who considered interfacial nano-layering and Brownian motion-induced convection. This was followed by Murshed et al.[22] in an attempt to derive a combined thermal conductivity model consisting of nanolayer, Brownian motion, surface chemistry and interaction potential elements. Xuan et al.[14] proposed a different thermal conductivity model that considers stochastic Brownian motion and nanoparticle aggregation, whilst Prasher et al.[24] combined aggregation kinetics with a Brownian motion-induced micro-convection model. The theoretical predictions of the latter model were later expanded to include nanofluid dependency on fluid chemistry and pH, time and viscosity effects[14, 25-27].

Additionally, when considering numerical simulations, most of the literature deals with nanofluids as a single-phase continuous fluid rather than a multi-phase system[2]. The single-phase approach assumes that continuum principles are still valid for the fluid. Here, it is assumed that suspended nano-sized particles follow the flow, and as such this methodology is simpler to implement and computationally much less expensive than explicitly resolving both phases. The alternative multi-phase technique better models each phase separately, however this method is not commonly used in the literature[17] due to its computational complexity and limitations associated with long compute

times. The latter technique is to be preferred when modelling nano-suspensions, as it is able to describe the key mechanisms and dynamic processes involved in such multiphase fluids.

There are a number of novel features in the model developed and described in this work. The parameters considered include particle size, physical interactions between the nanoparticles (collisions) and the dynamics between the particles and the carrier fluid, the particle surface (zeta) and related nanocolloidal properties. The significance of the enhanced thermophysical properties is considered, with emphasis on the solid-liquid characteristics (e.g. specific heat, thermal conductivity and coefficient of thermal expansion), and mechanical properties (e.g. modulus of elasticity, rigidity and Poisson's ratio), of the alumina ceramic nanoparticles (α-Al_2O_3, 71 nm diameter) in water. These characteristics are modelled dynamically as a function of temperature using data from Auerkari[28] in an attempt to understand the dynamics of nanoparticles in such multiphase systems. Ceramic oxide nanoparticles have been chosen for consideration in this study since they are available at reasonable commercial rates compared to other types of nanoparticles (e.g. carbon nanotubes and graphene), and hence are more likely to be adopted in practical systems. Additionally, α-Al_2O_3 ceramic nanoparticles possess strong ionic interatomic bonding giving an excellent combination of desirable thermophysical properties and thermal stability at elevated temperatures (i.e. usable in both oxidizing and reducing atmospheres up to 1900°C).

The kinetics of nanoparticles, such as aggregation, clustering and the resultant radius of gyration of the aggregates, are analysed using a depth-first search aggregate classification method. Finally, the thermal conductivity of nanofluids is predicted using an approach similar to that developed by Prasher et al.[14], but using a more justifiable Brownian velocity (by applying a Gaussian white noise process) for nanoparticles in a liquid rather than an approach based on the kinetic theory of gases.

Furthermore, the model is able to track the motion of embedded nanoparticles in the suspended

fluid, which is modelled using an Eulerian-Lagrangian hybrid scheme with fixed time stepping, based on the work of Fujita and Yamaguchi[29]. This approach enables quantification of the various multiscale forces (Brownian motion, particle collision, fluid drag and DLVO forces) whose characteristics (length and timescales) are quite different.

The study presented here improves and significantly extends previous preliminarily research[25]. First, the simulations are performed for significantly longer timescales in order to obtain more stable and converged predictions. The present work also includes: a validation of the computational model; further in-depth analysis to more comprehensively elucidate the key dynamics associated with thermal conductivity predictions; and significantly more results for the situations considered. As far as the authors are aware, there is no published analysis of the key dynamic factors affecting the stability and thermal conductivity of nanofluids using a similar multiscale computational modelling approach. Below, the combined mechanism-based model is described, and used to evaluate the most significant dynamic forces involved in nanofluids, with results and findings discussed. General conclusions are also drawn on the three-dimensional multiphase liquid-solid model's ability to predict aspects of thermal property enhancement in nanofluids, and their potential applications in industry.

Ultimately, the model can be used together with experimental investigations to provide more detailed insights into the fundamental dynamics of nanosuspensions, and can also be used in this regard in its own right. In addition, the present model allows different operating scenarios to be examined, and the impact of modifications to them established, again providing a better understanding of the particle dynamics, and hence the heat transfer characteristics of potential nanofluids. The final practical outcome is a model that can be used to establish the optimum characteristics for both coolants and thermal energy storage media.

THEORETICAL MODEL

The present section describes the governing equations solved in the computational model. The numerical technique developed in the present investigation describes each element of the solid phase as a computational sphere. The Lagrangian particle tracker solves the non-dimensional Newtonian equations of motion for each particle in order to calculate their trajectories (position and velocity at every computational timestep). The descriptive equation is derived by considering the force-balance between a particle's inertia and that of the fluid. The nanoparticle velocity, $\boldsymbol{u}_{NP} = (u_{NP}, v_{NP}, w_{NP})$, and the coordinates of particle position, $\boldsymbol{x}_{NP} = (x_{NP}, y_{NP}, z_{NP})$, vectors in the absence of particle rotation are given in the Lagrangian reference frame as[30]:

$$\frac{\partial\, \boldsymbol{x}_{NP}}{\partial\, t} = \boldsymbol{u}_{NP} \tag{1}$$

The motion of each nanoparticle is described using the Langevin equation[31], where the derivative of the translational velocity of the i-th particle is obtained from standard Newtonian dynamics:

$$m_p \frac{\partial \boldsymbol{u}_{NP,i}}{\partial t} = \boldsymbol{F}_i \tag{2}$$

where,

$$\boldsymbol{F}_i = \boldsymbol{F}_i^c + \boldsymbol{F}_i^e + \boldsymbol{F}_i^v + \boldsymbol{F}_i^f + \boldsymbol{F}_i^B \tag{3}$$

Here, m_p and $\boldsymbol{u}_{NP,i}$ are the mass and translational velocity vector of the i-th nanoparticle, respectively. $\boldsymbol{F}_i^c$ is the particle soft-sphere contact force; $\boldsymbol{F}_i^e$ the electric double layer repulsive force; $\boldsymbol{F}_i^v$ the van der Waals attractive force; $\boldsymbol{F}_i^f$ the fluid viscous drag force and $\boldsymbol{F}_i^B$ the stochastic Brownian motion force. Additional body forces such as gravity and buoyancy are assumed to be negligible for all length and time scales relevant to the present study, since their magnitudes are much smaller than the aforementioned inter-particle and hydrodynamic forces. The present model

predicts the dynamics and interaction mechanisms responsible for nanoparticle aggregation, including inter-particle collisions and DLVO (after Derjaguin and Landau[32], Verwey and Overbeek[33]) inter-particle van der Waals attraction and electric double layer repulsion forces[34], as well as fluid drag and Brownian motion forces. The fluid drag force is calculated based on the stagnant liquid in which the particles are suspended, and is proportional to the instantaneous particle velocity. In all simulations performed a Newtonian incompressible fluid with a constant kinematic viscosity is assumed. In this sense other carrier fluids can be considered via modification of the fluid parameters (viscosity and density). Furthermore, it is assumed that the drag force is dominant, which is realistic since only stagnant systems with a zero fluid velocity are considered. A soft-sphere approach is used to model inter-particle collisions as described by the Hertzian normal contact theory[35]. The model describes the collision force between the i-th and j-th spheres in the unit normal direction, $\boldsymbol{n}_{ij}$, according to the approach of Fujita and Yamaguchi[29], with a two-dimensional schematic given in Figure 1.

To predict inter-particle forces, DLVO theory is used, with intersurfacial separations considered down to 5 nm. These consist of a repulsive electric double layer force exerted between the two spheres, together with an attractive van der Waals forces that can be expressed mathematically[34] as:

$$\boldsymbol{F}_i^e + \boldsymbol{F}_i^v = \sum_j (f_{ij}^e + f_{ij}^v)\, \boldsymbol{n}_{ij} \tag{4}$$

The magnitude of the electrostatic repulsive force exerted between each of two homogeneously charged spheres can be determined using Derjaguin's approximation[34] using:

$$f_{ij}^e = -\frac{64\pi a n k_b T \Theta^2 e^{-\kappa H_{ij}}}{\kappa} \tag{5}$$

and for the attractive van der Waals forces[34]:

$$f_{ij}^{v} = \frac{Aa}{12H_{ij}^{2}} \tag{6}$$

with a the radius of a sphere; n the number density of electrolyte ions; k_b the Boltzmann constant; T the temperature; A the Hamaker constant; H the inter-particle distance (surface to surface) and Θ the polarizability factor, expressed as:

$$\Theta = \tanh\left(\frac{ze\zeta}{4k_bT}\right) \tag{7}$$

Here, κ is the Debye parameter (inverse of the Debye length), given as:

$$\kappa = \sqrt{\frac{2nz^2e^2}{\varepsilon_0\varepsilon_r k_b T}} \tag{8}$$

where z is the ion valence (a number representing ion concentration that is either a positive or negative integer); e the elementary electric charge; ζ the zeta potential of the nanoparticles; ε_0 the permittivity of a vacuum and ε_r the relative permittivity of the medium.

It should be noted that the magnitude of the van der Waals forces is limited below a maximum value to prevent divergence, thus the inter-surface distance is given a lower limit close to zero. These forces for two identically sized spherical particles are effective from a few angstroms to several hundred angstroms according to Butt[36]. Furthermore, Eqns. 4-7 are valid for $\kappa a < 5$, and so it is necessary to have a large Debye length for the medium, κ^{-1}, or small particle radius, a, such as occurs for nanoparticles in water. Moreover, these equations can only be applied for low electrolyte concentrations (i.e. salts and ionic liquids). Different expressions are available in the

colloidal literature for the repulsive force, for higher $\kappa a > 5$ values. For water-based nanofluids κ is relatively small and related to the concentration of ions, z, by[37]:

$$\kappa = 5.023 \times 10^{11}(z)^{0.5}/(\varepsilon_r T)^{0.5} \quad (9)$$

Equation (8), used in the present work, allows evaluation of κ for an aqueous solution at different values of electrolyte concentration and valence of ions, such that $z = 10^{-\mathrm{pH}}$ for pH ≤ 7 and $z = 10^{-(14-\mathrm{pH})}$ for pH > 7.

The Brownian force exerted on a spherical nanoparticle is modelled using a Gaussian white noise process given by Kim and Zydney[38]:

$$F^B = \xi \sqrt{\frac{12\pi a \mu_f k_b T}{\Delta t}} \quad (10)$$

in which ξ is the coefficient of Stokes drag for a sphere and μ_f is the dynamic viscosity of the fluid. The magnitude of the fluid force responsible for nanoparticle aggregation can be determined in a quiescent system using the following Stokesian equation[31]:

$$F^f = 6\pi a \mu_f \boldsymbol{u}_S \quad (11)$$

where $\boldsymbol{u}_S$ is the flow velocity relative to that of the particle ($\boldsymbol{u}_S = \boldsymbol{u}_F - \boldsymbol{u}_{NP}$). Here, $\boldsymbol{u}_F$ is the instantaneous fluid velocity at the location of the particle and $\boldsymbol{u}_{NP}$ is the particle velocity. To predict the overall heat transfer properties of the system, the above nanofluid dynamic model is further coupled to a thermal energy model, which works on the basis of inter-particle distances. These are tracked concurrently with the fluid phase at each timestep in the simulation. The volume of aggregates formed at each time step was calculated using a depth-first search method to iterate through aggregated particle chains and clusters. The applied technique links to the thermal model

by considering both Brownian motion (responsible for induced micro-convection) and aggregation kinetics (responsible for the formation of particle percolation pathways). These physical phenomena are both found to be responsible for modulating the effective thermal conductivity, k_{eff}, in nanofluids, as noted by Prasher et al.[14], and can be expressed mathematically as:

$$k_{eff} = (1 + C_A Re^m Pr^{0.333} \phi) \left\{ \frac{[k_{ag} + 2k_{bf} + 2(k_{ag} - k_{bf})\phi_{ag}]}{[k_{ag} + 2k_{bf} - (k_{ag} - k_{bf})\phi_{ag}]} \right\} k_{bf} \qquad (12)$$

where Re is the Brownian Reynolds number; Pr the Prandtl number, and C_A and m are constants determined from experiment; k_{ag} and k_{bf} represent the thermal conductivity of the particle aggregates and the base-fluid, respectively. The particle volume fraction is given by ϕ for a primary particle and as ϕ_{ag} for aggregated particles, which are characterized by their radius of gyration, R_a, determined using the depth-first search method, as illustrated in Figure 2.

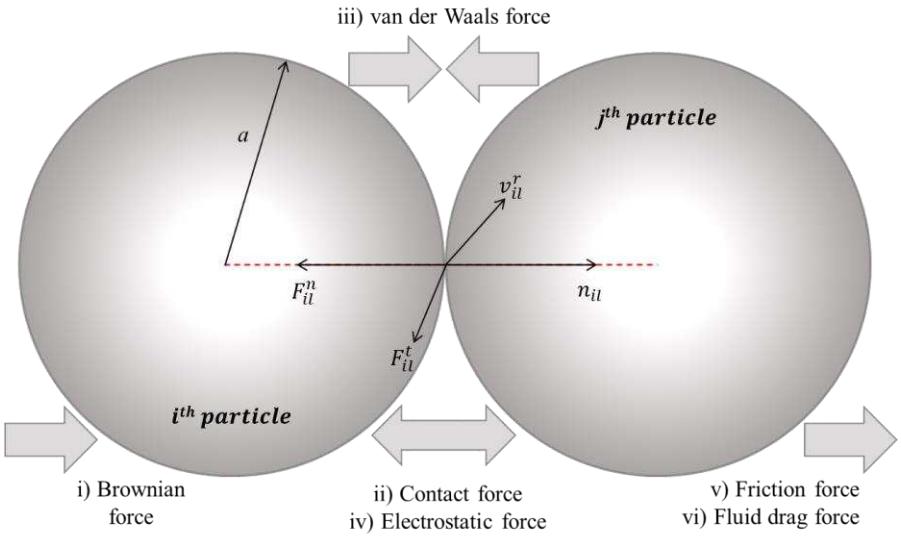

Figure 1. Hydrodynamic forces acting on two spherical solid particles submerged in a fluid continuum: (i) Brownian force; (ii) contact force; the instantaneous balance of the DLVO forces (iii) van der Waals and (iv) electrostatic; and the resulting (v) friction and (vi) fluid drag forces.

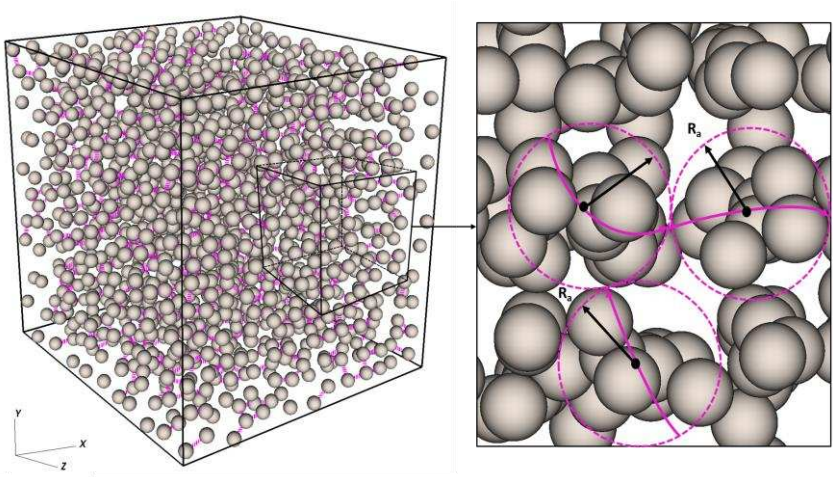

Figure 2. Schematic of aggregated particles in a three-dimensional computational cell (left). The aggregates are characterized by their radius of gyration (R_a) and shown to have a higher interacting mass than an individual nanoparticle (right), thereby creating a high conductivity percolation path.

COMPUTATIONAL METHOD

The multiscale model outlined in the previous section applies a Lagrangian particle tracking approach in order to investigate the heat transfer mechanisms in, and the dynamics of, nanofluids[25]. The three-dimensional computational region examined consists of a 1μm (i.e. $\Delta l = 1\times10^{-9}$ m) cube filled with stagnant water. This volume element contains a collection of 71 nm diameter Al_2O_3 spherical nanoparticles (40-2000 in number) that are initially located uniformly within the computational domain ensuring equal spacing between neighbouring particles. Periodic boundary conditions are applied in all directions. The dynamic properties of both phases are coupled to the ambient temperature of the fluid suspension, that being water at 25 to 85°C. The thermophysical characteristics of the multiphase system are also modelled dynamically, whereby the mechanical characteristic (e.g. modulus of elasticity, rigidity and Poisson's ratio) of the alumina ceramic nanoparticles in water change as a function of temperature [28].

The motion of the embedded nanoparticles in the fluid is treated using an Eulerian-Lagrangian hybrid scheme with fixed time stepping. To advect the particles, the equations of motion for

velocity and acceleration (Eqns. 1 and 2) are integrated using the fourth order Runge-Kutta algorithm with a very small time step, $\Delta t = 10^{-11}$ s, to fully capture the timescales associated with the short-range inter-particle forces of importance. The equation for acceleration is calculated using the relevant force terms in Eqn. 3. Each timestep, the terms in Eqn. 3 are recalculated using Eqns. 4 to 11, accounting for attractive and repulsive DLVO forces, inter-particle soft sphere collisions, Brownian forces and fluid viscous drag. Since there is no fluid flow, fluid velocity interpolation is unnecessary, and in Eqn. 11, which requires the local fluid velocity, this value is set to zero ($\boldsymbol{u}_F = 0$) to indicate a stagnant fluid. To determine whether soft-sphere collisions take place, a deterministic binary collision algorithm is used. The algorithm divides the domain into a coarse mesh, wherein overlapping particle pairs are searched for within each coarse cell. Finally, if a particle moves outside the fluid domain, it is reinjected into the corresponding location at the other side of the computational cube, satisfying periodicity. Model output is recorded each timestep and corresponding statistical quantities such as mean free path, particle velocities and inter-particle forces are calculated in post-processing.

RESULTS AND DISCUSSION

Various simulations were performed using the described model, with results analysed to determine the forces and mechanisms responsible for nanoparticle interaction dynamics, aggregation and subsequent thermal property enhancement. The spontaneous ordering process of the particles in the suspension was first examined, followed by clustering and agglomeration as a function of time. Timestep snapshots of the simulations at 5 vol. % are presented in Figure 3. Figure 3(a) presents the initial homogeneous distribution of single particles within the computational cell. Small aggregate clusters begin to form at later times, as in Figure 3(b), and subsequently large aggregates gradually form with increasing time (Figure 3(c)).

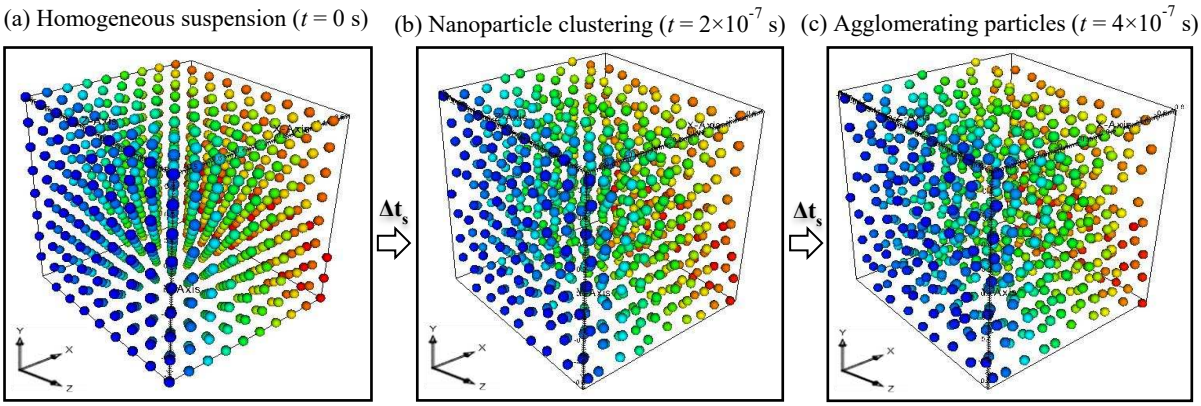

Figure 3. Representation of three-dimensional spherical 71 nm Al_2O_3 particles in 1 μm cubic cell filled with water showing: a) homogenous distribution of particles; b) formation of clusters; and c) nano-aggregation.

With the aim of investigating the influence of particle size on aggregation, the interaction of two suspended nanoparticles (with charged surfaces) was examined using three different sizes of particle, the results of which are presented in Figure 4.

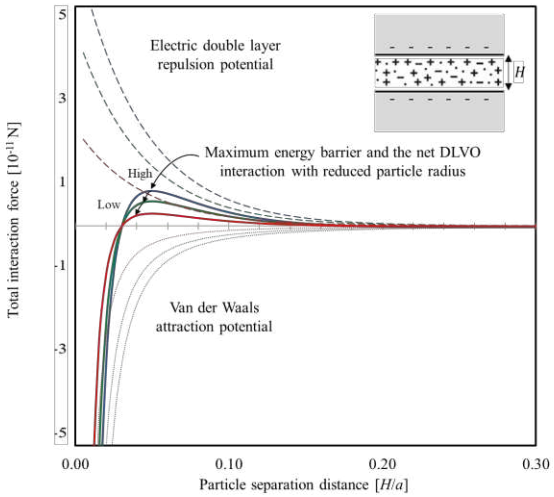

Figure 4. Interaction potential energy versus distance profiles of two colliding nanoparticles (spherical Al_2O_3 particles at 1 vol. % and 25°C) at three different sizes: 25 nm (red); 50 nm (green); and 71 nm (blue). Electric double layer (– –); maximum or total energy barrier (—) and van der Waals (···). The actual magnitude of the energy is proportional to the particle size (radius) or interaction area (between two planar surfaces).

The figure illustrates the potential energy of two colliding nanoparticles. For the different particle sizes used in the simulation it is clear that the electric double layer (long-range) force initially begins with an exponential decay. Then at smaller inter-particle distances, the attractive van der Waals (short-range) forces begin to dominate, leading to a collision between the two particles and

subsequent adhesion. In addition, for a constant volume fraction, aggregation increases with decreasing particle size as the average inter-particle distance between nanoparticles decreases. This is exemplified by the reduction in the potential energy observed for 71nm-sized particle as compared to 25nm-sized particles, where the maximum energy barrier (the sum of all the repulsive and attractive potentials) that the particles must overcome to collide and form an aggregate decreases with the reduction in size. These DLVO inter-particle interaction potentials were used to determine the size of nanoparticles required to optimise the simulation timestep and run length.

The model also allows for the magnitude of the different hydrodynamic and interaction forces exerted on nanoparticles in a suspension to be predicted, given a set of material and fluid properties. Figure 5 illustrates each of the multiscale forces plotted as a function of the intersurfacial distance, H, normalized by the particle radius, a. The results show the magnitude of the various forces exerted on the particles which drive particle collision and aggregation in the computational cell. They illustrate that when sufficient distance is maintained between nanoparticles, the effects of both the fluid (drag) and Brownian random motion forces dominate over other contributions since these forces are dependent on the velocity of the nanoparticles and interactions between the particles and the fluid. As the intersurfacial distance between particles becomes small ($H/a < 0.1$), the electric double layer repulsive force starts to have a significant effect on particle interactions. When two particles are close to colliding, the attractive van der Waals forces becomes dominant over all others. After a collision of two nanoparticles, the repulsive soft-sphere collision force increases rapidly and is of a similar magnitude as the attractive force.

The main conclusion is that the van der Waals attraction always exceeds double-layer repulsion at small enough separations since it represents a power law interaction, while the double-layer

interaction energy remains finite or rises much more slowly as the relative inter-particle distance tends to zero. These findings are in line with the existing literature on DLVO theory (i.e. Eqns. 4-6), as noted by Israelachvili[34] for the various types of interaction potential and the sequential phenomena that occur between two similarly charged or colloidal particles, and describe how the colloidal dispersion stability is affected by the electrolyte concentration and surface charge density.

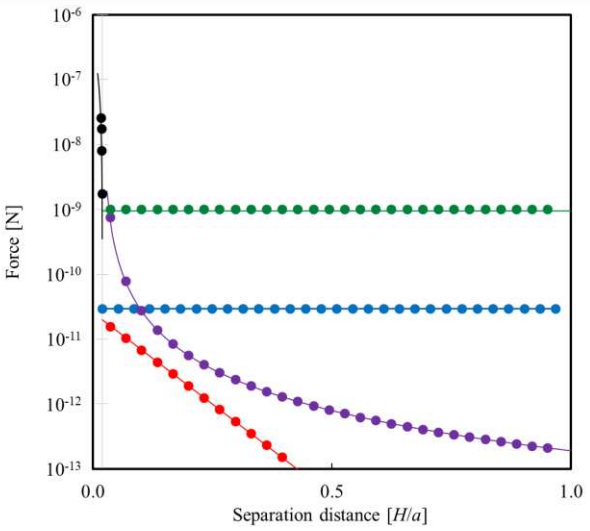

Figure 5. Validation of modelled colloidal forces across the control volume (1 μm cubic cell filled with water and spherical 71 nm Al_2O_3 particles at 1 vol. % and 25°C), showing the magnitude of the following forces: electric double layer (red); van der Waals (purple); fluid drag (blue); Brownian motion (green); and collision (black), as functions of inter-surface distance. Theory (—); and numerical (●).

The magnitude of the forces with inter-particle distance shown in Figure 5 leads to the conclusion that every force noted should be considered in the dynamic modelling of nanofluids, as they are all relevant at different interparticle separations. Moreover, the values given are in excellent agreement with similar results in the literature[29, 31]. The results of Figure 5 also confirm, and validate, the numerical implementation of the theory described above.

Interaction between nanoparticles and aggregate formation

The model allows for post-processing determination of the precise number of various dynamic events. Firstly, collision events are defined to be an event in which two particles 'intersect' and

then separate whilst soft-sphere interaction forces are active. The mean free path between particles along with aggregate number (using the depth-first search to identify chains of particles) can then be calculated. Figure 6 provides predictions of the average number of aggregates formed in the system as a function of solid volume concentration and temperature, together with mean free path values.

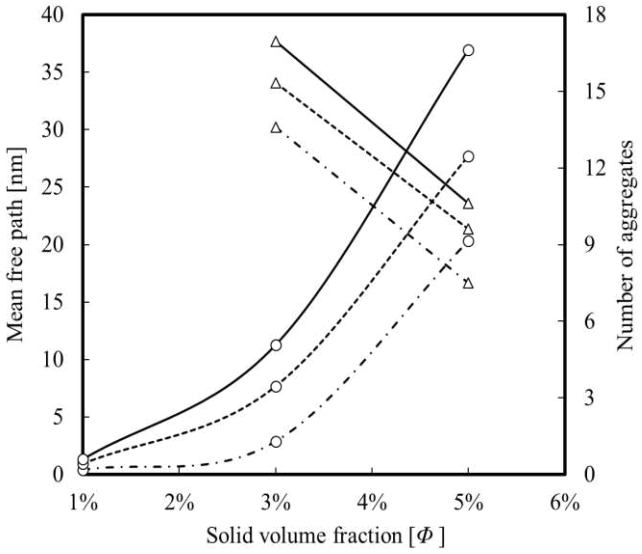

Figure 6. Number of aggregates (○) and mean free path (△) versus particle concentration: at 25°C (- · -); 55°C (----); and 85°C (—).

It is clear from the results of Figure 6 that very few aggregates are formed when the concentration is 1 vol. %, and so the mean free path predictions are not shown for this case. At 3 vol. %, the mean free path clearly decreases due to collisions and agglomerations. Above 3 vol. %, the system enters a regime where both collisions and agglomerations begin to take place more frequently, leading to a substantial increase in the mean number of aggregates. The probability of collision and aggregation increases with increasing temperature due to the effect of Brownian motion. In terms of the fundamental dynamics, it is clear that particles at increased temperatures exhibit an increased mean free path, and therefore cover a larger distance in the same period of time, increasing their collision cross section, which further increases the aggregation rate.

Corresponding results for the nanoaggregate mean radius of gyration, R_a, were determined using the depth-first search method, described earlier. The results are presented in Figure 7, together with predicted effective thermal conductivity, k_{eff}, values, at different volume fractions and temperatures.

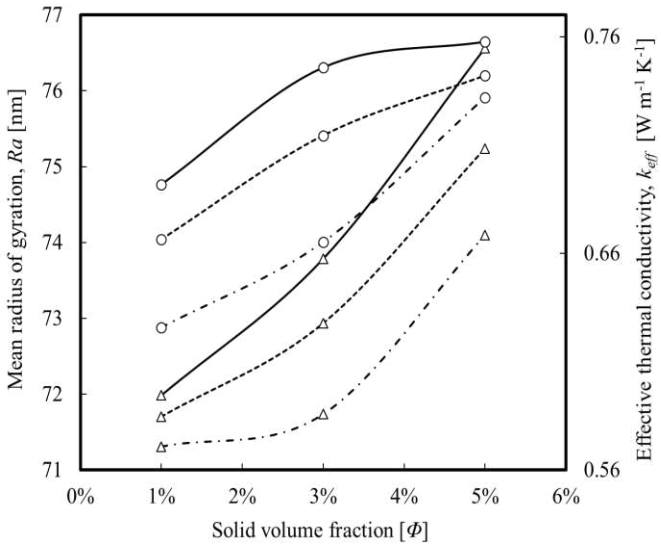

Figure 7. Mean radius of gyration (△) and thermal conductivity (○) versus particle concentration: at 25°C ((- · -); 55°C (----); and 85°C (—).

The results for the thermal conductivity given in Figure 7 show an almost 13% increase in k_{eff} for 5 vol. % of particles over the solid volume fraction range considered. These predictions were made over a temperature range of 25 to 85 °C, and show that enhancement is to be expected. The exhibited temperature dependency is likely a result of increased kinetic energy and hence fluid drag and Brownian motion forces, encouraging collisions and providing more chances for aggregation. Although the Brownian motion force decreases as the mass of aggregates increases over time, the increase in k_{eff} is still evident, as highly conducting ceramic nanoparticles come in contact with each other. Thus, with increasing collisions and aggregation with time, the concentration and temperature variations indicate the effect of direct particle contact and the agglomerates' percolation effects on the conductivity. The observed combined effects of

convection and conduction on thermal enhancement in nanofluids have been reported by Prasher et al.[14], and are of the same magnitude as exhibited in the results of Figure 7. This leads to the same conclusion regarding the percolation effect in nanoaggregates and the dominant dynamic forces which are believed to govern thermal behaviour in nanofluids. The other interesting behaviour in the trend in conductivity is that it tends to plateau at concentrations of 3 vol. %, and temperatures of 55°C, and above, which can be explained by the simultaneous increase in the mass of the aggregates and the decrease in the nanoparticles' Brownian motion. As might be anticipated, the predicted mean radius of gyration of the aggregates increases significantly with both the solid volume fraction and temperature, although the temperature dependence is lower for increased volume fractions, likely due to the reduced interparticle separation reducing the necessity for increased particle speeds to instigate collisions.

Effect of time on aggregate radius of gyration

As noted, analysis of the size distribution of nanoparticle aggregates within the computational cell shows that there is a significant dependency of the nanoaggregates' mean radius of gyration, R_a, on temperature and solids concentration. Figure 8 presents the time sequence of R_a values over 400 ns of simulation time at 25 to 85 °C. At a given time point it is clear that a rise in temperature results in an increase of the nanoaggregate size. This occurs at all concentrations, but most significantly at 5 vol. %.

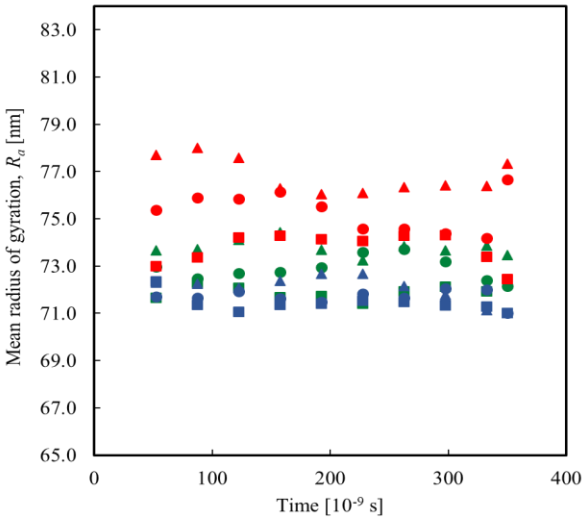

Figure 8. Time dependence of aggregate mean radius of gyration at: 25°C (■); 55°C (●); and 85°C (▲); and for 1 vol. % (blue); 3 vol. % (green); and 5 vol. % (red).

Aggregation is known to be a time-dependent phenomenon. Similar conclusions as those noted can be reached from the nanoaggregate size distribution inferred from R_a values over time, as shown in Figure 9, which gives the trend of the aggregate mean radius of gyration for the 3 vol. % and 5 vol. % concentrations at three different temperatures between 25 and 85°C. The temperature dependence of R_a is quite evident from the increase in the relatively stable time dependent R_a values with temperature.

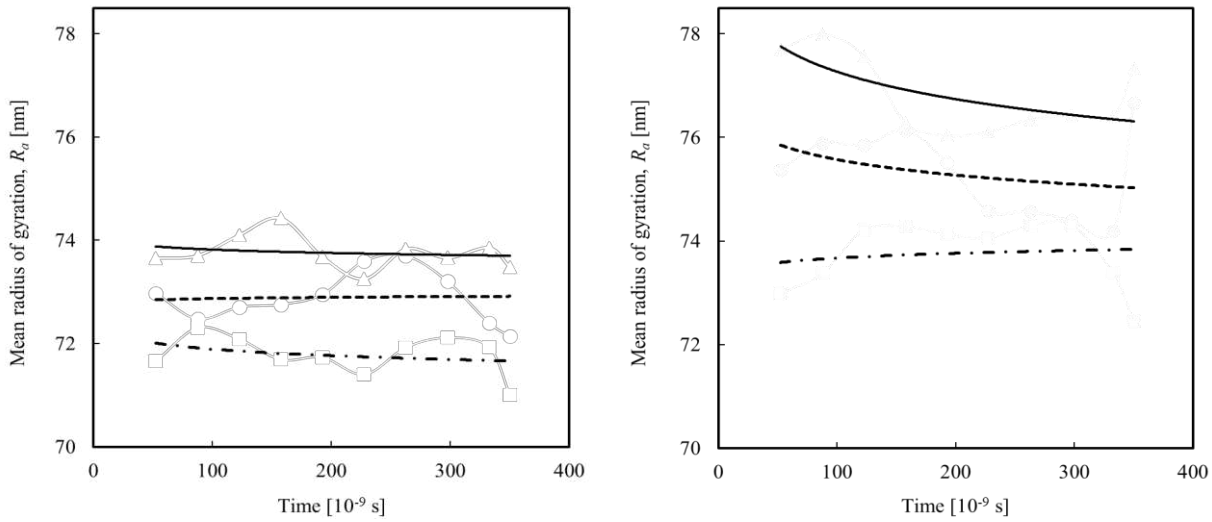

Figure 9. Variation of mean radius of gyration with time. The figure shows the variation in R_a for the 3 vol. % concentration (left) and 5 vol. % concentration (right): 25°C (- · -); 55°C (----); and 85°C (—).

Effect of temperature and concentration on thermal conductivity

The great potential for thermal conductivity enhancement using nanofluids has encouraged many researchers to undertake comprehensive investigations using various methods and techniques. The thermal conductivity values predicted by the present model are therefore compared against relevant experimental measurements and other model predictions from a number of sources[39-42], with good agreement found. This comparison is shown in Figure 10, with both the data and predictions from the latter sources showing the same trend in thermal conductivity enhancement with increasing volume fraction of nanoparticles as the present model.

FFigure 10 10 gives predictions made by Nan et al.[41] that account for the effects of particle size, shape, distribution, volume fraction, the orientation of inclusions and the interfacial thermal resistance on the conductivity of particulate composites. In addition, their model was developed in terms of an effective medium approach combined with a Kapitza-type thermal contact resistance to reflect the thermal conductivity of composites made up of arbitrary ellipsoidal inclusions embedded in an imperfect matrix-inclusion. This may explain the discrepancy between predictions of their model and those of the present work since the Nan et al.[41] model characterizes the conductivity of particulate composites within an interfacial thermal resistance without accounting for all the possible mechanisms involved and the dynamic forces present in nanofluids.

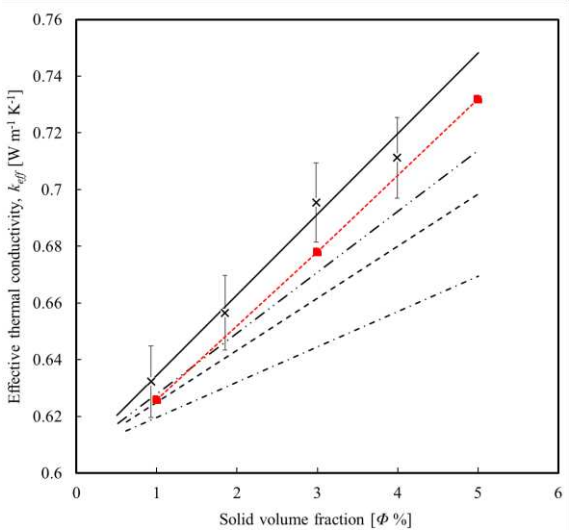

Figure 10. Effective thermal conductivity of nanofluids containing spherical 71 nm Al_2O_3 particles as a function of volume fraction Φ. Experimental data of Beck et al.[39] (×), with error bars from that source. Theoretical work of Maxwell[40] is shown for a spherical nano-suspension (– –). Lines represent predictions of Nan et al.[41] (– · –), Yu and Choi[11] (– · · –), Warrier et al.[42] (—) and the present model (--■--).

The theoretical values of the static model of Maxwell[40] presented in Figure 10 lie slightly below the predictions of the present model. This classical model is widely used to determine the effective electrical or thermal conductivity of liquid-solid suspensions of monodisperse, low volume fraction mixtures of spherical particles. However, it originated from a continuum formulation that typically involves only the particle size and shape, and volume fraction, and assumes diffusive heat transfer in both the fluid and solid phases. Therefore, even if it does give good predictions for micro-metre or larger-size multiphase systems, the model generally underestimates the magnitude of thermal conductivity enhancement in nano-suspensions as a function of volume fraction[17].

The predictions of Yu and Choi[11] were derived using a modified version of the Maxwell equation which includes the effect of liquid molecules close to the solid surface of nanoparticles on the thermal conductivity of solid-liquid suspensions. This effect assumes the formation of layered solid-like structures (known as ordered nanolayers) which have a major impact on nanofluid conductivity[11], in particular when the particle diameter is less than 10 nm. Although their

predictions are found to be slightly below the results derived from the present model, they follow the same overall trend and are found to be remarkably similar.

Also shown in Figure 10 are measurements from the pioneering experimental research of Beck et al.[39] who, amongst others, elucidated the behaviour of heat conduction in nanofluids. Their study used seven sizes of spherical alumina nanoparticles ranging from 8 to 282 nm in diameter, with results indicating that the thermal conductivity enhancement decreases as the particle size decreases below approximately 50 nm. The authors attributed this effect to a decrease in the thermal conductivity of the nanoparticles themselves (as the particle size becomes small enough to be affected by increased phonon scattering). The measurements also showed a clear effect of the particle size and method of dispersion, and indicate that there is a limiting value to the thermal conductivity enhancement for nanofluids containing large particles. This limit was found to be greater than that predicted by the Maxwell equation, but could be predicted well using the volume fraction weighted geometric mean of the bulk thermal conductivities of the two phases. Their results show some nonlinearity of the thermal conductivity with respect to particle concentration, and although they are found to be marginally above the predictions of the present study the latter generally lie within the error bars attributed to the measurements.

Warrier et al.[42] also modelled the thermal conductivity of nanoparticle suspensions and examined the effect of the two phases present in the heterogeneous system. Their model takes into account adjustable parameters such as the temperature dependence of the thermal conductivities of the individual phases, as well as the size dependence of the dispersed phase. Using this modified version of the geometric mean model allowed the effect of a wide range of particle sizes (11 to 302 nm), volume fractions and temperatures to be studied. The model is also capable of predicting the effect of different base fluids and the decrease in the thermal conductivity of semiconductor

nanoparticles, especially when the particle size is of the same order as the phonon mean free path. Although the predictions of Warrier et al.[42] given in Figure 10 are slightly above the present results, they have approximately the same rate of increase in conductivity with increasing solid volume fraction.

It can be concluded that experimental measurements and model predictions of nanofluid thermal conductivity generally fit between the lower and upper mean-field bounds originally proposed by Maxwell[40], with the static configurations of nanofluid conductivity ranging between the two extremes of a dispersed phase and a continuous phase, as explained by Kleinstreuer and Feng[43]. However, it should be noted that dynamic models of nanofluid thermal conductivity represent an enhancement of classic Maxwell theory and thereby provide additional physical insight into the phenomena considered. Undoubtedly, it is necessary to consider not only one possible mechanism but combine several in order to explain enhancement in the thermal conductivity of nanofluids.

With the aim of verifying these predictions, values of the normalized thermal conductivity, k_{eff} / k_{bf}, are plotted against temperature and volume fraction in Figure 11. The results show that the present conductivity values are in reasonable agreement with experimental data and the predictions made by the other researchers noted. In particular, the obtained values are remarkably similar to the predictions of Das et al.[44] at the same operating temperature of 25 ^{o}C, as well as with predictions of the spherical model of Hamilton and Crosser[6]. The probability of combined collision and aggregation increases linearly as the concentration increases from 1 vol. % to 3 vol. %. The other interesting aspect of the results is observed at 3 vol. % and above, where a change in the slope of the conductivity values with increasing volume fraction is evident. This demonstrates that the system is entering a different regime were collisions driven by Brownian motion start to weaken

and instead agglomeration starts to dominate, leading to the substantial increase in conductivity values.

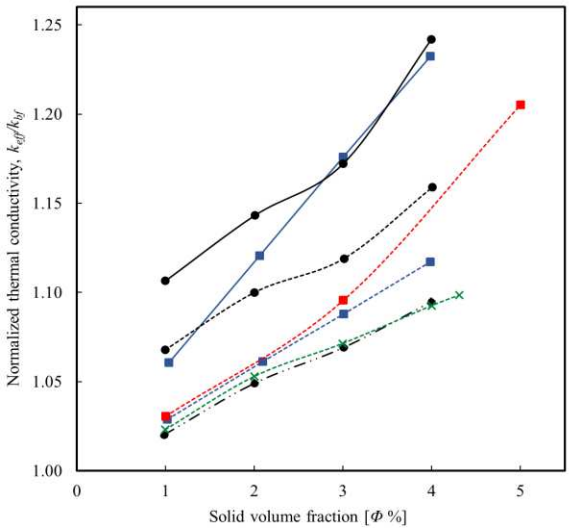

Figure 11. Thermal conductivity ratio of Al_2O_3 nanofluids at different solid concentrations. Experimental data of Lee et al.[45] at 21°C (--×--). Lines represent the predictions of Das et al.[44] at 25°C (– · · –●), 33°C (--●--) and 51°C (–●–). The theoretical work of Hamilton and Crosser[6] at 21°C is shown for both cylindrical (–■–) and spherical (--■--) models. Predictions of the present model at 25°C (--■--).

The approximately linear relationship between the thermal conductivity and temperature, and particle concentration, is another behaviour that is predicted by the model, as illustrated in Figure 12. It is clear from these results that the temperature dependence is not as strong at concentrations < 3 vol. %, but for larger values a stronger dependence is apparent. This reflects the role of intermolecular forces, dominated in this case by Brownian motion, that are strongly temperature- and concentration-dependent[42]. A similar increase in the normalized thermal conductivity with temperature has also been reported by Das et al.[44], and is thought to be caused by the stochastic motion of the nanoparticles. Figure 12 also shows the effect of the volume concentration of nanoparticles on thermal conductivity enhancement: it increases with volume concentration from 1 to 5 vol. % of nanoparticles. Similar effects have been reported for different nanofluids based on experimental measurements and model predictions[11, 39, 42, 45]. The thermal conductivity

enhancement in nanofluids at higher concentrations is believed to be due to the increased interaction of nanoparticles in the base fluid, and the interactions that occur as more nanoparticle chains are formed. The same figure also illustrates the variation in thermal conductivity enhancement with respect to temperature (ranging from 25°C to 85°C). The maximum conductivity was obtained at 85°C and the enhancements are 4%, 6.7% and 25% for 1 vol. %, 3 vol. % and 5 vol. %, respectively, compared with pure water. The thermal conductivity is enhanced at higher temperatures due to Brownian motion and collisions between nanoparticles[46].

Similar results were obtained by Prasher et al.[24], in agreement with the previously explained combined mechanism-based model of aggregation kinetics with Brownian motion-induced micro-convection. These findings support the superiority of nanofluid dynamic models as they take the effect of the nanoparticles' random motion into account, while static models assume that the nanoparticles are stationary relative to the base fluid, which is not physically realistic.

For the nanofluids considered, k_{eff} was found to increase with temperature over the range 25 to 85°C. This can be seen from the simulation results presented in Figure 13.

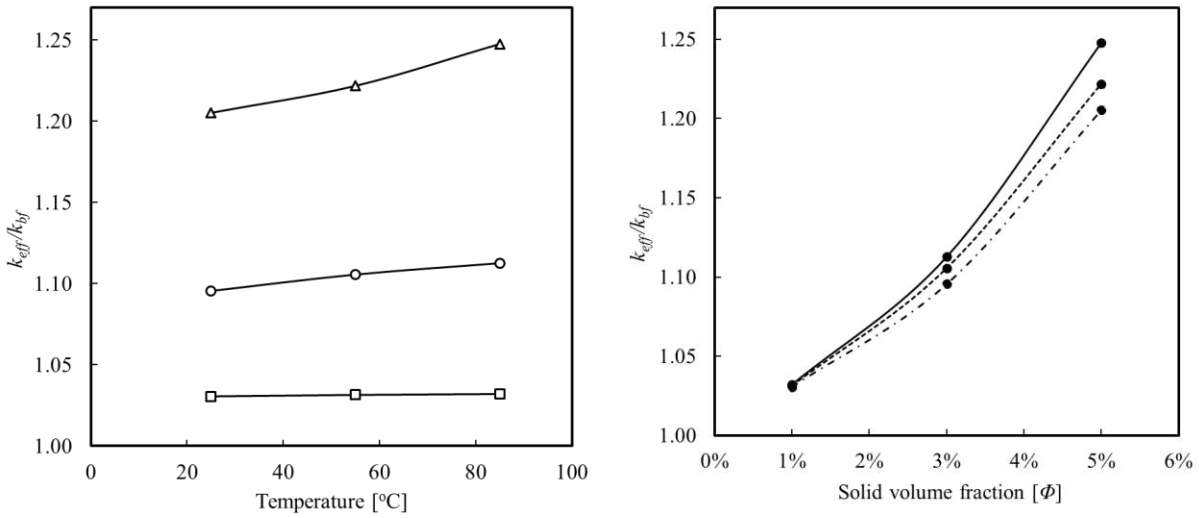

Figure 12. Normalized thermal conductivity enhancement as a function of temperature (left) at: 1 vol. % (–□–); 3 vol. % (–○–); and 5 vol. % (–△–), and as function of concentration (right) at: 25°C (– · –); 55°C (----); and 85°C (—).

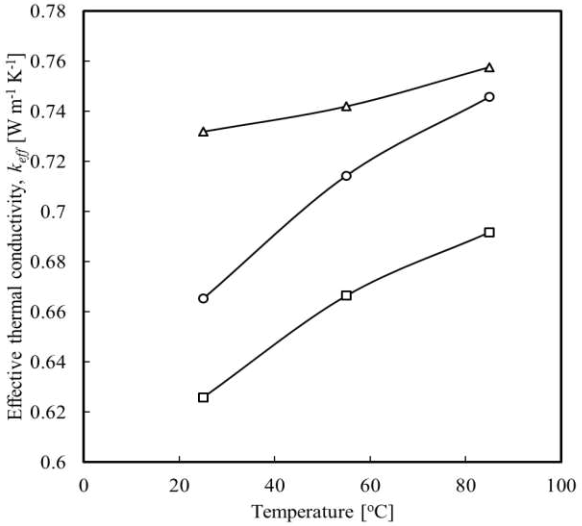

Figure 13. Effective thermal conductivity enhancement as function of temperature at: 1 vol. % (–□–); 3 vol. % (–○–); and 5 vol. % (–△–).

Similar behaviour was reported by Das et al[20], who noted that the variation in the thermal conductivity of the nanofluid with temperature closely follows that of the base fluid. To investigate this observation, the present simulations were extended to cover a wider range of temperatures than previously considered, from 0 to 100°C, and the results, together with values of the conductivity of pure water and Al_2O_3, are compared in Figure 14.

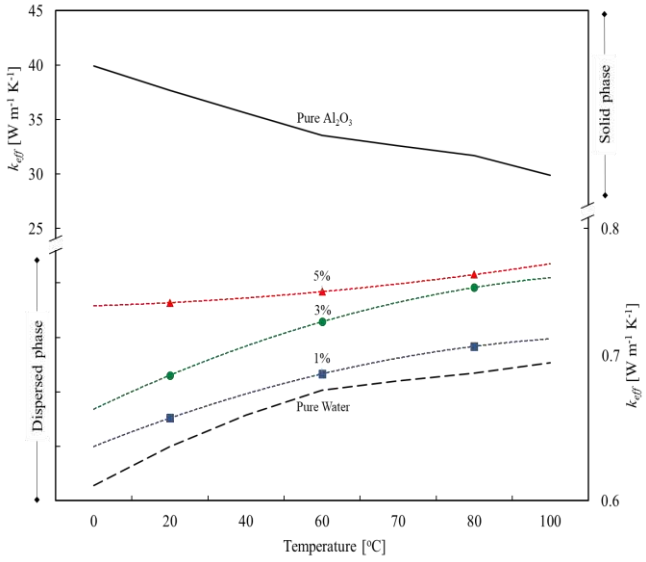

Figure 14. Predictions of thermal conductivity as a function of temperature at: 1 vol. % (--■--); 3 vol. % (--●--); and 5 vol. % (--▲--). Lines represent standard reference data for pure water of Ramires et al.[49] (– –) and experimental data for pure aluminium oxide of Touloukian[50] (—).

It can first be noted that the gradual increase in the conductivity of pure water, such as that reported by Ramires et al.[49], from the hydrogen bonded structures could, to a large extent, be responsible for the increase in k_{eff} in water-based nanofluids at relatively low particle concentrations of around 1 vol. %. Also, research has shown that k_{eff} for pure water is relatively high and rises to a maximum value at approximately 130°C, starting to fall at higher temperatures[47]. A partial decrease in k_{eff} with increasing temperature is therefore expected above this value, even when other types of base-fluids are used. For instance, for oil-based nanofluids the thermal conductivity of oil is expected to decrease with increasing temperature, and so the overall k_{eff} of the mixture will be slightly affected[48]. Adding additional nanoparticles to the mixture could compensate for the drop in thermal conductivity caused by the base fluid.

Secondly, the general trend in the nanofluid conductivity shows an increase in k_{eff} with temperature as the particle concentration increases up to 3 vol .% which is qualitatively in line with the trend for pure water. Above this value, however, the k_{eff} variation with temperature begins to move away from that observed for pure water to more closely resemble that observed for pure solid Al_2O_3. The conductivity of pure solid Al_2O_3 decreases with an increase in temperature, an effect due to the gradual accompanying phase change. This implies that the mechanism for thermal conductance in nanofluids at high concentrations above 5 vol. % will likely move away from the liquid mixture behaviour and become more similar to that of pure solid composites, as described by Keblinski et al.[8].

Effect of pH variation of nanofluid on thermal conductivity

The thermal conductivity of the nanofluids considered was found to be highly dependent on changes in pH which is one of several important factors that determine the isoelectric point of a nano-suspension (as it varies the surface potential and hence controls the magnitude of the repulsive force), with this point defined as the pH at which the surface of the nanoparticles exhibit a neutral net electrical charge or, equivalently, a zero zeta potential, i.e. $\zeta = 0$ V. For this particular value of ζ, only attractive van der Waals forces are significant, and the solution is not stable as the repulsive forces between particles tend to decrease to zero. This is referred to as the point of zero charge, for which a colloidal particle is found to be electro-kinetically uncharged leading to poorer dispersion and increases in particle attraction and agglomeration[20, 51]. In this study, established isoelectric point values from experimental investigations on colloids were employed to provide guidance for model development[14, 52]. Thus, the pH value corresponding to the isoelectric point of an Al_2O_3-water nanofluid has been determined[53] to occur at pH ≈ 8.5 - 9.2 (for α-Al_2O_3, purity > 99.9%, suspensions). Similar values were reported by Kim et al.[54] for α-Al_2O_3 suspensions with ζ potentials ranging from -55 mV at a maximum pH = 10.5, 22 mV at pH = 7, and 75 mV at pH = 1. Clearly, an increase in pH lowers the zeta potential in a ceramic α-Al_2O_3 nano-suspension.

The dynamics of nanoparticle suspensions are affected by all the parameters noted earlier, including those related to the DLVO energy profile. Correspondingly, nanoparticle stability and agglomeration in the present model is controlled by changing the ionic concentration valence, z. As such, a variation from 1 to 5 in z is representative of a change in pH from neutral or acid (pH ≤ 7), which promotes stability, to values outside the region of the isoelectric point at pH ≈ 8.5 - 9.2. Figure 15 gives predictions of the conductivity against pH values, and with respect to R_a and Φ, demonstrating the strong pH-dependence of the system. This is equivalent to changing the

valency which changes the Debye length (the screening potential), with a high valency corresponding to high screening, hence poor stability (i.e. more aggregation).

From the figure it can be seen that the range of electrostatic surface potentials decreases as the valence of the ions in solution increases. This demonstrates that the dispersion of Al_2O_3 is affected by the electrostatic repulsion force which is in agreement with classical DLVO theory. Regarding the increase in thermal conductivity due to percolation effects (direct contact between the particles) in the aggregates, this effect is also illustrated in the results of Figure 15 where a clear enhancement in conductivity values occurs as a function of pH at a given temperature and concentration.

The results in the figure also clearly indicate the thermal conductivity enhancement due to the combined effect of collision and aggregation as concentration increases from 1 vol. % to 3 vol. %, in line with Equation (12). Another interesting feature of the results is the shift observed at concentrations of 4 vol. %, where a change in the ionic concentration valence from 1 to 5 causes a rise in the conductivity from 0.70 to 0.735 $Wm^{-1}K^{-1}$. An increase in conductivity values at higher volume fractions is evident, but when the system is forced to form aggregates (by moving away from the isoelectric point), it enters a different regime. Up to that point, collisions driven by Brownian motion had begun to diminish and instead agglomeration had started to dominate, leading to the substantial increase in conductivity values observed, resulting from percolation effects and heat transfer by conduction through the nanoaggregates. Nevertheless, at concentrations $\geq$ 5 vol. % the system enters a limiting region, where a clumped nano-suspension (congested aggregates) starts to form due to the presence of too many nanoparticles in the control volume. This demonstrates that although aggregation can enhance the conduction contribution compared to a well-dispersed system, it needs to be controlled to ensure the formation of well dispersed aggregates (chain-like clusters), rather than large congested aggregates.

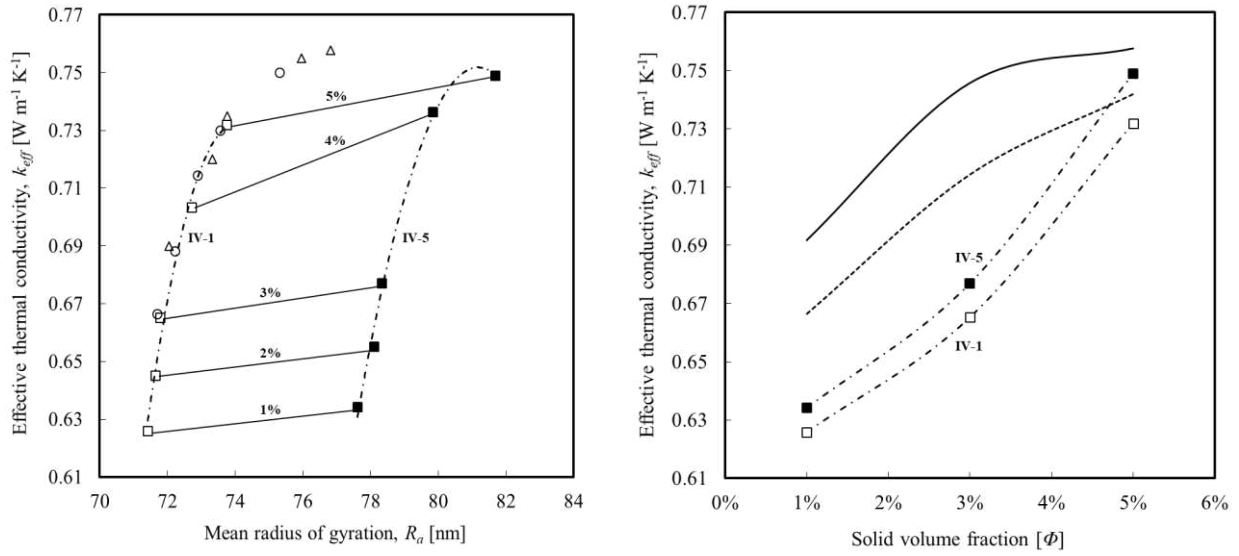

Figure 15. Thermal conductivity dependence on the mean radius of gyration (left) – effect of pH presented as a function of changes in z from $z = 1$ corresponding to pH ≤ 7 (– · □ · –) to $z = 5$ outside of the isoelectric point at pH ≈ 8.5-9.2 (– · ■ · –) at 25°C (□); 55°C (○); and 85°C (△). Note that R_a is higher at the isoelectric point as energy potential for alumina at this pH reaches zero. Thermal conductivity dependence on solid volume fraction (right) – dependence is represented at different ion valencies IV-1 (– · □ · –) and IV-5 (– · ■ · –) at 25°C against particle concentration, and: ion valency IV-1 at 55°C (----); and 85°C (—).

Figure 15 also shows that the thermal conductivity increases with an increase in particle concentration, as well as with the difference between the pH value of the aqueous suspension and the isoelectric point of Al_2O_3 particles. It can clearly be seen that at 25°C, and at 1 vol. % to 3 vol. %, the change in pH (screening potential) is still significant even if the system is optimally aggregated. Thus, a slight change in pH leads to a clear enhancement in the thermal conductivity of the system. At higher concentrations ≥ 4 vol. % the effect of full nanoparticle aggregation leads to combined convective and conductive effects and hence an improved thermal conductivity. Conversely, at higher concentrations (≥ 4.5 vol. %) the thermal conductivity curve starts to flatten and the effect of increasing pH causes the 25°C curve to overlay the 55°C curve. This leads to the conclusion that at higher concentrations the effects of Brownian motion are reduced and instead percolation effects dominate due to increased nanoparticle aggregation in the system.

In general, the numerical simulations indicate that a change in zeta potential (determined in part by the valence and pH of the solvent phase) is an important parameter as it affects the level of agglomeration in nanofluids. Similar behaviour in ceramic nano-suspensions was reported by Lee et al.[55] who studied the effect of the surface charge on the thermal behaviour of nanofluids. The study indicated that this basic parameter is primarily responsible for the thermal conductivity enhancement of nanofluids. It also highlighted how colloidal nanoparticles can be destabilized as the pH of the solution moves closer to the isoelectric point, eventually altering the thermal conductivity of the nanofluid. It is concluded that the pH of the colloidal liquid strongly affects the suspension stability and hence the performance of thermal nanofluids.

CONCLUSIONS

Key variables related to the stability and thermal conductivity of nanofluids have been examined using multiscale simulations. The novel model developed enables the prediction of the various dynamic forces acting in nanofluids, and provides quantitative predictions of the magnitude of those forces, including their role in particle aggregation. The model has been found to perform well in comparison with similar studies, and provides predictions of nanofluid dynamic properties, including the effect of the base fluid, and nanoparticle characteristics such as size[56], concentration, temperature, pH and external driving forces, on the thermal conductivity of the system.

The model provides confirmation of the effect of temperature and concentration on the enhancement of thermal conductivity. In addition, high temperatures are found to enhance nanoparticle interactions, collisions and aggregation which, ultimately, can inhibit higher conductivities in nanofluids. Such increases in conductivity are desirable for practical applications of nanofluids, for example if they are to be used in thermal applications. With regards to nanoparticle concentration, at low loadings (< 1 vol. %) it appears that the effective conductivity

is dominated by that of the base fluid. However, at moderate concentrations (≈ 3 vol. %) the thermal conductivity enters a zone of intensive interactions between nanoparticles, with the combined effects of aggregation (responsible for conduction) together with Brownian motion-induced convection governing the conduction of heat in the system. At higher concentrations (≥ 5 vol. %) the system starts to behave in a fashion more akin to that found in pure solid composites. This leads to the conclusion that the conductivity of nano-suspensions is dependent on the physical properties of the nanoparticles and their interactions, including the interaction between nanoparticles and the liquid, and the conductivity of the base fluid and nanoparticle material.

These new findings, not previously predicted through multiscale simulation, also demonstrate the importance of particle agglomeration and how it leads to extended pathways (chain-like clusters) with a higher effective thermal conductivity. The impact of aggregate structures is therefore found to be positive in terms of the conduction of heat. However, aggregation into sparse but large clusters is known to increase the viscosity of the fluid and can become significant when the aggregates start to touch one another [8, 27, 57]. For this reason, nanoaggregates may not be as favourable in some practical applications involving fluid flow, if high viscosity is of concern. To overcome this, appropriate physical and surface charge modifications can be implemented, using pH adjustment, to ensure that the level of nanoparticle aggregation always remains under control.

In terms of limitations, the present model only applies to stagnant fluids (as it is computationally expensive to solve for the fluid phase evolution), simple geometries and limited numbers of particles. Future work will extend the model's application to include other base-fluids such as ionic liquids and molten salts (used as hydride nanofluids for thermal energy storage applications), and to flow situations by coupling the tracking approach described with direct numerical simulations. This will involve optimization of the properties of the nanofluid by considering different

nanoparticle materials, and different particle sizes, shapes and concentrations. Experimental research will also be conducted to support the development of this numerical model – to track, characterise and model the dynamics and thermal enhancement of potential nanofluids. Further research initiatives in this area will assist in the design of renewable-energy power plants and other thermal management systems that involve nanofluids.

AUTHOR INFORMATION

Corresponding Author: *bgy9bm@leeds.ac.uk; **ORCID iD: https://orcid.org/0000-0002-7647-0119; Bashar Mahmoud:** 0044-7762-086868

Author Contributions

B.M. conceived the study. M.F., J.P, D.H and H.R. supervised the study. B.M. and L.M performed the numerical calculations. All authors analyzed the results, discussed their implications, wrote the paper and revised the manuscript at all stages.

ACKNOWLEDGMENT

The authors wish to thank the Kuwait Institute for Scientific Research (KISR) for its financial support of this work.

REFERENCES

1. Choi, S.U.S. Nanofluids: From Vision to Reality Through Research. J. Heat Transfer **2009**, 131, 033106/1– 033106/9.
2. Wang, X.Q.; Mujumdar, A.S. A Review on Nanofluids – Part I: Theoretical and Numerical Investigations. Braz. J. Chem. Eng. **2008**, 25, 613– 630.
3. Wang, X.Q.; Mujumdar, A.S. A Review on Nanofluids – Part II: Experiments and Applications. Braz. J. Chem. Eng. **2008**, 25, 631– 648.

4. Kole M.; Dey T.K. Thermal conductivity and viscosity of Al2O3 nanofluid based on car engine coolant. J Phys D: Appl Phys **2010**, 43, 315501.
5. Masoumi, N.; Sohrabi, N.; Behzadmehr, A. A new model for calculating the effective viscosity of nanofluids, J. Phys. D: Appl. Phys. **2009**, 42 874– 885.
6. Hamilton, R.L.; Crosser, O.K. Thermal Conductivity of Heterogeneous Two-Component System. Industrial and Engineering Chemistry Fundamentals **1962**, 1, 187– 191.
7. Hashin, Z.; Shtrikman, S.A. Variational Approach to the Theory of the Effective Magnetic Permeability of Multiphase Materials. Journal of Applied Physics **1962**, 33, 3125– 3131.
8. Keblinski, P.; Prasher, R.; Eapen, J. Thermal Conductance of Nanofluids: Is the Controversy Over?. Journal of Nanoparticle Research **2008**, 10, 1089– 1097.
9. Eapen, J.; Rusconi, R.; Piazza, R.; Yip, S. The Classical Nature of Thermal Conduction in Nanofluids. ASME Journal of Heat Transfer **2010**, 132, 102402.
10. Keblinski, P.; Phillpot, S.R.; Choi, S.U.S.; Eastman, J.A. Mechanisms of Heat Flow in Suspensions of Nano-Sized Particles (Nanofluids). International Journal of Heat and Mass Transfer **2002**, 45, 855– 863.
11. Yu, W.; Choi, S.U.S. The Role of Interfacial Layers in the Enhanced Thermal Conductivity of Nanofluids: A Renovated Maxwell Model. J. Nanoparticle Research **2003**, 5, 67– 171.
12. Yu, C.-J.; Richter, A.G.; Datta, A.; Durbin, M.K.; Dutta, P. Molecular Layering in a Liquid on a Solid Substrate: An X-ray Reflectivity Study. Physica B: Condensed Matter **2000**, 283, 27– 31.
13. Nagvenkar, A. P.; Perelshtein, I.; Gedanken, A. Doping Effect on the Thermal Conductivity of Metal Oxide Nanofluids: Insight and Mechanistic Investigation. J. Phys. Chem. C **2017**, 121, 26551– 26557.
14. Prasher, R.; Phelan, P.E.; Bhattacharya, P. Effect of Aggregation Kinetics on the Thermal Conductivity of Nanoscale Colloidal Solutions (Nanofluid). Nano Letters **2006**, 6, 1529– 1534.
15. Feng, Y.; Yu, B.; Xu, P.; Zou, M. The Effective Thermal Conductivity of Nanofluids Based on the Nanolayer and the Aggregation of Nanoparticles. Journal of Physics D: Applied Physics **2007**, 40, 3164– 3171.
16. Das, S.K.; Choi, S.U.; Patel, H.E. Heat Transfer in Nanofluids – A Review. Heat Transfer Eng. **2006**, 27, 3– 19.

17. Lee, S.-H.; Jang, S.P. Mechanisms and Models of Thermal Conductivity in Nanofluids, in Heat Transfer Enhancement with Nanofluids, Bianco, V.; Manca, O.; Nardini, S.; Vafai, K. (Eds.). CRC Press, Boca Raton, Florida, 2015, 78– 98.
18. Wang, X.Q.; Xu, X.; Choi, S.U.S. Thermal Conductivity of Nanoparticle Fluid Mixture. J. Thermophys. Heat Tr. **1999**, 13, 474– 480.
19. Jang, S.P.; Choi, S.U.S. Role of Brownian Motion in the Enhanced Thermal Conductivity of Nanofluids. Appl. Phys. Lett. **2004**, 84, 4316– 4318.
20. Das, S.K.; Choi, S.U.S.; Yu, W.; Pradeep, T. (Eds.). Nanofluids: Science and Technology, John Wiley & Sons, Hoboken, New Jersey, 2008.
21. Ren, Y.; Xie, H.; Cai, A. Effective Thermal Conductivity of Nanofluids Containing Spherical Nanoparticles. J. Phys. D: Appl. Phys. **2005**, 38, 3958– 3961.
22. Murshed, S.M.S.; Leong, K.C.; Yang, C. A Combined Model for the Effective Thermal Conductivity of Nanofluids. Appl. Therm. Eng. **2009**, 29, 2477– 2483.
23. Xuan, Y.; Li, Q.; Hu, W. Aggregation Structure and Thermal Conductivity of Nanofluids. AIChE J. **2003**, 49, 1038– 1043.
24. Prasher, R.; Bhattacharya, P.; Phelan, P.E. Thermal Conductivity of Nanoscale Colloidal Solutions (Nanofluids). Phys. Rev. Lett. **2005**, 94, 025901/1– 025901/4.
25. Mahmoud, B.H.; Fairweather, M; Mortimer, L.F.; Peakall J.; Rice, H.R.; Harbottle, D. Prediction of stability and thermal conductivity of nanofluids for thermal energy storage applications. Computer-Aided Chem. Eng. **2018**, 43, 61– 66.
26. Prasher, R.; Evans, W.; Meakin, P.; Fish, J.; Phelan, P.; Keblinski, P. Effect of Aggregation on Thermal Conduction in Colloidal Nanofluids. Appl. Phys. Lett. **2006**, 89, 143119/1– 143119/3.
27. Prasher, R.; Song, D.; Wang, J.; Phelan, P. Measurements of Nanofluid Viscosity and its Implications for Thermal Applications. Appl. Phys. Lett. **2006**, 89, 133108/1– 133108/3.
28. Auerkari, P. Mechanical and Physical Properties of Engineering Alumina Ceramics. Technical Research Centre of Finland, ESPOO, 1996.
29. Fujita, M.; Yamaguchi, Y. Multiscale Simulation Method for Self-Organization of Nanoparticles in Dense Suspension, J. Comput. Phys. **2007**, 223, 108– 119.
30. Mortimer, L.; Fairweather, M.; Njobuenwu, D.O. Particle Concentration and Stokes Number Effects in Multi-Phase Turbulent Channel Flows. 5th International Conference on Particle-Based Methods, Hannover, Germany: **2017**, 859– 869.

31. Sloan, G.; Feng, Z.-G.; Bhaganagar, K.; Banerjee, D. Coupled Direct Numerical Simulation and Experimental Approach to Develop Framework for Nanofluids. ASME International Mechanical Engineering Congress and Exposition, Houston, USA: **2012**, 7, 2877– 2882.
32. Derjaguin, B.; Landau, L. Theory of the Stability of Strongly Charged Lyophobic Sols and of the Adhesion of Strongly Charged Particles in Solutions of Electrolytes. Acta Physicochim. **1941**, 14, 633– 662.
33. Verwey, E.J.W.; Overbeek, J.T.G. Theory of the Stability of Lyophobic Colloids. J. Colloid Sci. **1955**, 10, 224– 225.
34. Israelachvili, J.N. Intermolecular and Surface Forces, Academic Press, Elsevier, London, 2011.
35. Timoshenko, S.P.; Goodier, J.N. Theory of Elasticity, 3rd Ed., McGraw-Hill, New York, 1970.
36. Butt, H.-J.; Kappl, M. Surface and Interfacial Forces, Wiley VCH, 2009.
37. Hiemenz, P. C. Principles of Colloid and Surface Chemistry, Marcel Dekker, New York, 1997.
38. Kim, M.; Zydney, A.L. Effect of Electrostatic, Hydrodynamic, and Brownian Forces on Particle Trajectories and Sieving in Normal Flow Filtration. J. Colloid Interface Sci. **2004**, 269, 425– 431.
39. Beck, M.P.; Yuan, Y.; Warrier, P.; Teja, A.S. The Effect of Particle Size on the Thermal Conductivity of Nanofluids. J. Nanopart. Res. **2009**, 11, 1129– 1136.
40. Maxwell, J. C. A Treatise on Electricity and Magnetism, 3rd Ed., Clarendon Press, Oxford, 1892.
41. Nan, C.W.; Birringer, R.; Clarke, D.R.; Gleiter, H. Effective Thermal Conductivity of Particulate Composites with Interfacial Thermal Resistance. J. Appl. Phys. **1997**, 81, 6692– 6699.
42. Warrier, P.; Yuan, Y.; Beck, M.P.; Teja, A.S. Heat Transfer in Nanoparticle Suspensions: Modeling the Thermal Conductivity of Nanofluids; AIChE J. **2010**, 56, 3243– 3256.
43. Kleinstreuer, C.; Feng, Y. Experimental and Theoretical Studies of Nanofluid Thermal Conductivity Enhancement: A Review. Nanoscale Res. Lett. **2011**, 6, 1– 13.
44. Das, S.K.; Putra, N.; Thiesen, P.; Roetzel, W. Temperature Dependence of Thermal Conductivity Enhancement for Nanofluids. J. Heat Transfer **2003**, 125, 567– 574.
45. Lee, S.; Choi, S.U.S.; Li, S; Eastman, J.A. Measuring Thermal Conductivity of Fluids Containing Oxide Nanoparticles. J. Heat Transfer **1999**, 121, 280– 289.

46. Hojjat, M.; Etemad, S.G.; Bagheri, R.; Thibault, J. The Thermal Conductivity of Non-Newtonian Nanofluids, 8th World Congress of Chemical Engineering, Montreal, Canada, 2009.
47. Kell, G. S. Thermodynamic and Transport Properties of Fluid Water, in Water A Comprehensive Treatise, Vol. 1, F. Franks (Ed.), Plenum Press, New York, 1972; 363– 412.
48. Sridhara, V.; Satapathy, L.N. Effect of Nanoparticles on Thermal Properties Enhancement in Different Oils – A Review. Critical Reviews in Solid State and Material Sciences **2015**, 40, 399– 424.
49. Ramires, M.L.V.; Nieto de Castro, C.A.; Nagasaka, Y.; Nagashima, A.; Assael, M.J.; Wakeham, W.A. Standard Reference Data for the Thermal Conductivity of Water. J. Phys. Chem. Ref. Data **1995**, 24, 1377– 1382.
50. Touloukian, Y.S. Thermophysical Properties of High Temperature Solid Materials. Macmillan, New York, 1967.
51. Xie, H. Q.; Wang, J. C.; Xi, T. G.; Liu, Y.; Ai, F.; Wu, Q. R. Thermal Conductivity Enhancement of Suspensions Containing Nano-Sized Alumina Particles. J. Appl. Phys. **2002**, 9, 4568– 4572.
52. Yopps, J. A.; Fuerstenau, D. W. The Zero Point of Charge of Alpha-Alumina, J. Colloid. Sci. **1964**, 19, 61– 71.
53. Singh, B.P; Menchavez, R.; Takai, C.; Fuji, M.; Takahashi, M. Stability of Dispersions of Colloidal Alumina Particles in Aqueous Suspensions. J. Colloid Interface Sci. **2005**, 291, 181– 186.
54. Kim, D. J.; Kim, H.; Lee, J. K. Dependence of the Rheological Behavior of Electrostatically Stabilized Alumina Slurries on pH and Solid Loading. J. Mater. Sci. **1998**, 33, 2931– 2935.
55. Lee, D. J.; Kim, W.; Kim, B. G. A New Parameter to Control Heat Transport in Nanofluids: Surface Charge State of the Particle in Suspension, J. Phys. Chem. B **2006**, 110, 4323– 4328.
56. Ganesan, V.; Louis, C.; Damodaran, S.P. Novel nanofluids based on magnetite nanoclusters and investigation on their cluster size-dependent thermal conductivity. J. Phys. Chem. C **2018**, 122, 6918– 6929.
57. Kwak K.; Kim, C. Viscosity and Thermal Conductivity of Copper Oxide Nanofluid Dispersed in Ethylene Glycol. Korea-Aust. Rheol. J. **2005**, 17, 35– 40.